Efficient Power Conversion Using a PV-PCM-TE System Based on a Long Time Delay Phase Change With Concentrating Heat

Ning Wang, Jian Tang, Heng-Sheng Shan, Hong-Zhi Jia, Run-Ling Peng, and Lei Zuo

***Abstract*—Based on the characteristics of phase change concentrated heat, this article proposes a photovoltaic/phase change/thermoelectric (PV-PCM-TE) self-supply system with sidewall integrated TE. In the system, an intelligent control circuit for phase change time is designed to intelligently switch the TE working mode using real-time temperature tracking. Therefore, the phase change time of the phase change material (PCM) is delayed with enhanced heat absorption and storage capacity, resulting in greater suppression of the PV temperature rise. Based on the constant temperature difference during the delayed phase change, more electrical power output can be obtained with integrated multistage thermoelectric generators (TEGs) in the sidewall of the PCM container. With the supplementary TEG energy injected into the PV battery, a complete self-powered design is constructed, leading to improved system energy efficiency. Experimental results show that compared with the PV-PCM-TEG system, the PCM phase change time of the proposed system is extended by 15 min, where the peak PV temperature after suppression is only 68.5 °C, which is 8 °C lower than that of the conventional PV-TEG-PCM system. The conversion efficiency of the entire system reached 30.26%, an improvement of 43.15%. The proposed self-powered PV-PCM-TE power conversion system with a long-time delay and high efficiency can operate during both day and night, providing a green scheme for intelligent low-power electrical systems.**

***Index Terms*—Intelligent switching, phase change heat accumulation, photovoltaic/phase change/thermoelectric (PV-PCM-TE) system, thermal conductivity.**

Manuscript received 21 December 2022; revised 11 April 2023; accepted 3 June 2023. Date of publication 6 June 2023; date of current version 28 July 2023. The work of N. Wang was supported in part by the Shanghai Natural Science Foundation under Grant 21ZR1446300, in part by the Key Laboratory of Wide Band-gap Semiconductor Materials, Ministry of Education, Xidian University, under Grant kdxkf2020-02, in part by the Natural Science Basic Research Program of Shaanxi under Grant 2021JM-384, in part by the NSFC under Grant 61804096, in part by the National Key Research and Development Program of China under Grant 2018YFA0701800, and in part by the Chengfeng project for conducting visiting research at Virginia Tech. The work of J. Tang, H.-S Shan, H.-Z Jia, and R.-L Peng was supported in part by the Shanghai Natural Science Foundation under Grant 21ZR1446300, in part by the Key Laboratory of Wide Band-gap Semiconductor Materials, Ministry of Education, Xidian University, under Grant kdxkf2020-02, in part by the Natural Science Basic Research Program of Shaanxi under Grant 2021JM-384, in part by the National Natural Science Foundation of China under Grant 61804096, and in part by the National Key Research and Development Program of China under Grant 2018YFA0701800. The work of L. Zuo was supported by the National Science Foundation under Grant 1915946. Recommended for publication by Associate Editor K. Kim. *(Corresponding authors: Run-Ling Peng; Lei Zuo.)*

Ning Wang is with the Engineering Research Center of Optical Instrument and System, Ministry of Education, Shanghai Key Laboratory of Modern Optical System, University of Shanghai for Science and Technology, Shanghai 200093, China, and with the Center for Energy Harvesting Materials and Systems, Virginia Tech, Blacksburg, VA 24061 USA, and also with the Shanghai Shenshou Semiconductor Technology Company, Ltd., Shanghai 201203, China (e-mail: nwang@usst.edu.cn).

Jian Tang, Hong-Zhi Jia, and Run-Ling Peng are with the Engineering Research Center of Optical Instrument and System, Ministry of Education, Shanghai Key Laboratory of Modern Optical System, University of Shanghai for Science and Technology, Shanghai 200093, China (e-mail: charles_tj@163.com; hzjia@usst.edu.cn; pengrunling@usst.edu.cn).

Heng-Sheng Shan is with the Materials Institute of Atomic and Molecular Science, Shaanxi University of Science and Technology, Weiyang University Park, Xi'an 710021, China (e-mail: hsshan@sust.edu.cn).

Lei Zuo is with the Center for Energy Harvesting Materials and Systems, Virginia Tech, Blacksburg, VA 24061 USA (e-mail: leizuo@vt.edu).

Color versions of one or more figures in this article are available at https://doi.org/10.1109/TPEL.2023.3283301.

Digital Object Identifier 10.1109/TPEL.2023.3283301

I. Introduction

MOST of the world's energy consumption comes from nonrenewable sources such as fossil fuels [1], [2], [3], [4]. However, energy extraction from fossil fuels brings pollution and energy waste [5], [6], which has a large impact on global warming and climate. A feasible way to solve this problem is to create clean energy [7]. Solar energy is one of the most renewable and potential energy sources that is currently available. Solar energy is a renewable energy source that can be obtained free of charge and used anywhere [8]. Solar energy can also be converted into electrical energy through the photovoltaic effect [9], reducing the excessive dependence on fossil fuels and having a strong potential to reduce energy consumption and carbon emissions [10]. However, photovoltaic (PV) systems cannot convert all solar energy into electricity, and a lot is released as heat, which also leads to energy efficiency degradation due to a high-temperature environment [11]. Therefore, it is an attractive and challenging problem to develop waste heat utilization to improve the conversion efficiency of PV systems [12].

The combination of PV panels and thermoelectric generator (TEG) is built into a hybrid PV-TEG system, which can improve the energy conversion efficiency. Yin et al. conducted a comprehensive experimental optimization of a PV-TEG system, established an experimental system with an adjustable light source, and verified the feasibility of the PV-TEG system with an efficiency increase of 8.7% [13]. Wang et al. designed a PV-TEG system with efficient thermal management and an intelligent switching circuit. Using this novel circuit, the PV temperature decreased by 4 °C with a 15.65% increase in energy conversion efficiency [14]. Although the energy conversion efficiency of the PV-TEG system can be improved to some extent, the PV temperature was still not well controlled along with most accumulated

waste heat in the system. Phase change materials (PCMs) have high latent heat and can be used in different working temperature ranges with different melting points ranging from 10 °C to 51 °C [15], [16], [17]. When the PCM reaches its phase change condition, it will absorb a lot of heat while maintaining a constant temperature (i.e., the phase change temperature). Therefore, PCMs are often used for passive heat storage and temperature control, which is well suited for heat dissipation in PV systems [18], [19], because the PV cell temperature can be reduced because the heat released in the PV system will be absorbed in the case of the use of PCM. In addition, TEGs can also be used to waste heat reuse, which increases the conversion efficiency of the entire system with the generated electricity [20]. When the PCM and TEG operate together, a stable power output from the TEG can be ensured when the temperature difference between the sides of the TEG remains relatively constant due to the fixed surrounding temperature supplied by the PCM phase change [21]. At night, the heat stored in the PCM during the daytime will also be released and converted into electrical energy by the TEG, improving energy utilization [22]. For example, Darkwa et al. investigated the architecture of an integrated thermoelectric PCM into PV cells and evaluated the effect of thicker PCM layers on PV junction temperature. The built PV/TEG/PCM system suppressed a 2.2 °C temperature rise in the PV panels in natural air conditions compared to the one in standard PV and achieved a 9.5% increase in power output [23]. Because the PCM in this system is not in direct contact with the PV cell where the heat is most concentrated, its potential for heat absorption due to phase change is not fully achieved, resulting in its ability to suppress PV temperature rise being somewhat low. The PV and PCM as the hot end and cold end of the TEG, respectively, effectively maintain a steady decrease in the temperature overnight, resulting in the TEG having difficulty creating a large temperature difference and thus more power. As a result, the TEG cannot make good use of the waste heat in PCM, particularly at night. Thus, a new structural PV-PCM-TEG system is proposed with enhanced solar intensity using two reflectors with angles facing the sun, where PCM is directly attached to the PV cell surface [24]. Electricity can still be generated at night using this structure, which is also converted from the stored heat in the PCM on the TEG. The power generation and PV cell efficiency of the system are increased by 100% and 1.38%, respectively; and the temperature of the PV cell is markedly reduced from 74.43 °C to 53.72 °C. However, the system phase transition time is short, the final conversion efficiency improvement is limited, and this system does not achieve intelligent thermal tracking and is fully self-powered.

In this article, a new system structure of PV-PCM-TE with intelligent regulation is proposed. The system intelligently switches the working mode of the TE module according to the real-time tracking of PV temperature to effectively extend the phase change time of the PCM. The system completes the energy conversion at night and is self-powered, which markedly improves the conversion efficiency of the entire system.

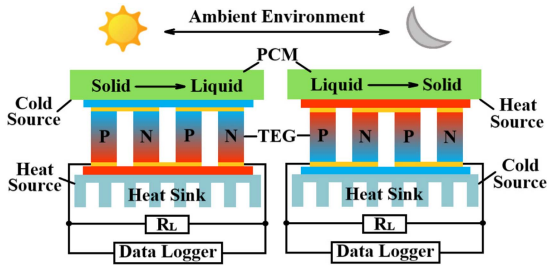

Fig. 1. Schematic diagram of the basic application of energy storage and power generation for PCMs.

The rest of this article is organized as follows. Section II provides an introduction to the theory of PCM, TEG and TEC. The design process of the PV-PCM-TE system is provided in Section III. Then, the experimental results are discussed and analyzed in Section IV. Finally, Section V concludes the article.

II. Principle and Theory

Combining PCM with TEG, Fig. 1 shows the application architecture of power generation using the storing energy technique, driving TEG to operate with the temperature difference formed by the state transformation of PCM during daytime and nighttime. This system consists of a PCM, a TEG, and a heat sink. In this article, the TEG is placed between the PCM and the heat sink. The constant temperature is maintained with PCM by storing and releasing large amounts of heat, which creates better conditions for TEG electricity generation with switched polarity between daytime and nighttime. Some studies have provided TEG with a power generation temperature difference of approximately 6 °C–8 °C through PCM phase transition, which can last for 35–50 min [25], [26], [27]. In our work, When the ambient temperature is 24 °C and the illumination is 5000 lux, the maximum temperature difference between the two sides of the TEG module in the system can reach 10 °C. If PCM uses paraffin wax with a phase change temperature of 38 °C and a latent heat value of 220J/Kg, the stable temperature difference on both sides of TEG can be maintained for about one hour. The application of PCM as a heat absorbing storage module in a TEG will effectively extend the energy endurance, reduce energy loss, and help improve the energy conversion efficiency of the entire system.

A. Phase Change Material

PCM is a material that can change the state of the substance itself at a constant temperature, accompanied by latent heat inside. Latent heat is the energy absorbed or released by a substance changing from one phase to another under isothermal and isobaric conditions. The process of transforming physical properties is called the phase change process when the PCM absorbs or releases latent heat. The calculation of latent heat of PCM can be described as

$$Q_c = mE_c \tag{1}$$

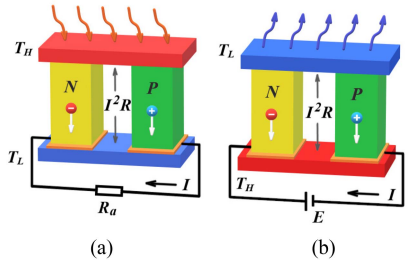

Fig. 2. (a) Single-stage TEG. (b) Single-stage TEC.

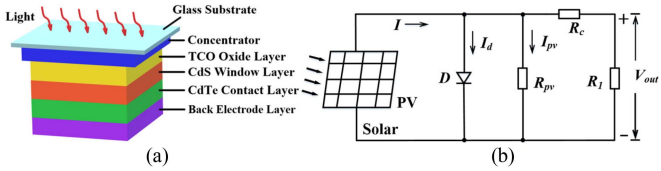

Fig. 3. (a) PV structure. (b) PV equivalent circuit.

where m is the mass of the PCM and E_c is the enthalpy change value of the material. During phase change, the PCM conducts heat exchange with the outside to achieve the purpose of endothermic temperature control and energy utilization. Compared with sensible thermal energy storage, phase change energy storage has the advantages of small size, high energy storage, constant temperature control, and a wide range of phase change temperature selection. Thus, PCM combined with TEG can act as both a heat source and a cold source for the TEG, promoting secondary energy use. During the day, PCM absorbs a lot of heat from the environment as the ambient temperature rises. When the temperature of the PCM rises to the phase change temperature, the PCM undergoes a phase change and keeps its own temperature constant. At this time, the PCM acts as a cold source with the heat sink as a heat source, and then, a large temperature difference between the two sides of the TEG can be created, leading to the generation of more electrical power. At night, the energy in the PCM will be released into the environment to maintain a constant phase change temperature when the ambient temperature drops to the melting point of the PCM. During phase change, the temperature of the PCM will be higher than that of the heat sink. Thus, the PCM acts as a heat source with the heat sink as a cold source, allowing the TEG to generate secondary electricity at night [22]. Therefore, the application architecture using PCM shown in Fig. 1 can harvest energy both day and night, providing a premise to improve energy utilization efficiency.

B. Thermoelectric Devices

Thermoelectric technology enables the conversion of thermal energy into electrical energy and vice versa. As a solid-state direct energy conversion technology, TEGs can use both the Seebeck effect for electricity generation and the Peltier effect for cooling [28], [29], [30]. As shown in Fig. 2, the basic structure of a thermoelectric conversion device is a Π-type element consisting of a p-type thermocouple arm and an n-type thermocouple arm connected in thermal parallel and electrical series. When there is a temperature difference applied by the two ends of a thermoelectric arm, the holes at the hot end gain higher energy, producing more holes relative to the cold end. The difference in the concentration of holes causes them to undergo diffusive motion, creating a spatial electric field or potential difference within the material. Under the effect of this potential difference, an opposite drifting charge flow is also formed inside the material. When the two reach a dynamic equilibrium, a stable temperature difference electric potential is formed at both ends of the material. Fig. 2(a) shows a single-stage TEG, which is a thermoelectric conversion device formed by two thermoelectric arms of n-type and P-type sandwiched between insulating, thermally conductive ceramic plates. Assuming that the hot end temperature of the upper ceramic plate and the cold end temperature of the lower ceramic plate are T_H and T_L, respectively, then there will be a potential difference between the two couple arms when T_H and T_L are not equal according to the Seebeck effect:

$$V_{np} = S_{np}(T_H - T_L) \tag{2}$$

where S_{np} is the Seebeck coefficient of the n and p coupling arms. If the total resistance of the two electrocoupled arms is R and the load resistance is R_a, the loop current and output power can be expressed as:

$$I_{np} = \frac{S_{np}(T_H - T_L)}{R + R_a} \tag{3}$$

$$P_{teg} = I_{np}^2 R_a = \left[\frac{S_{np}(T_H - T_L)}{R + R_a}\right]^2 R_a. \tag{4}$$

Energy harvesting converts thermal gradients into electrical energy through a TEG [31], and the power output of a TEG depends on the temperature difference loaded on its hot and cold sides [32]. The technical data for TEG device used in this article is TEP1-126T200 [33]. Fig. 2(b) shows a single-stage thermoelectric cooler (TEC) with a structure similar to that of a TEG. The applied voltage V across the thermocouple arms is equal to the voltage drop V_R across the thermocouple arms plus the voltage drop V_{np} required to overcome the Seebeck voltage

$$V = V_R + V_{np} = IR + S_{np}(T_H - T_L). \tag{5}$$

Therefore, the input power of the TEC can be described as follows:

$$P_{tec} = I^2 R + S_{np}(T_H - T_L)I. \tag{6}$$

C. Photovoltaic Cell

Fig. 3(a) shows a schematic diagram of the composition of a conventional PV cell. In PV cells, electrical energy can be directly converted from light energy through internal photoelectric and chemical effects. The glass substrate is penetrated by sunlight and reaches the light gathering layer. The concentrated sunlight reacts in the TCO layer, which is a transparent conductive oxide layer equivalent to an electrode. Then, the light passes through the CdS window layer (n-type semiconductor)

and the CdTe contact layer (*p*-type semiconductor) to reach the back contact layer of the back electrode, which is used to reduce the contact barrier between CdTe and the metal electrode. Fig. 3(b) shows the internal equivalent circuit diagram of the PV cell. When the PV cell absorbs solar radiation, the output current I is generated by the photovoltaic effect, and the real internal current I_d flows through the diode during operation. Thus, energy loss will be generated due to the resistance R_c, which is connected in parallel with the internal resistance R_{pv} of the *P–N* junction material to form the total internal resistance $R_{0,}$ and R_1 is the load resistance. However, the material of the battery determines the internal resistance. Considered together, the total energy absorbed by the solar energy through the PV cell can be expressed as:

$$P_0 = CL\varepsilon\tau S \tag{7}$$

where C is the concentration ratio of the internal material of PV; L is the radiation intensity of the sun; ε and τ are the transmittance and absorption of light of the PV cell, respectively; and S is the effective area of the PV cell receiving light. The conversion efficiency of a PV cell is related to the internal material properties, the external environment, temperature, and other factors [34]. From the internal equivalent circuit diagram of a PV cell, it shown that there is an intrinsic resistance of the PV cell. The resistance of the internal resistance changes with the external temperature, and the intrinsic heat loss also fluctuates. Therefore, the relationship between the conversion efficiency of the PV cell and its own material and temperature is as follows:

$$\eta_{\text{pv}} = \eta_0[1 - \lambda(T_{\text{pv}} - T_0)] \tag{8}$$

where η_0 is the cell efficiency of the PV cell at T0 = 24.85 °C, which is determined by the intrinsic cell material; T_{pv} is the instantaneous temperature of the PV cell; and λ is the temperature coefficient of the conversion efficiency of the PV cell. Additionally, the external temperature has a strong influence on the conversion efficiency of the PV cell. From (7) and (8), we can deduce that the total output power of the PV cell is

$$\begin{aligned} p_{\text{pv}} &= p_0\eta_{\text{pv}}\frac{R_1}{R_0 + R_1} \\ &= p_0\eta_0[1 - \lambda(T_{\text{pv}} - T_0)]\frac{R_1}{R_0 + R_1}. \end{aligned} \tag{9}$$

The total output power of the PV cell is proportional to the conversion efficiency of the cell and inversely proportional to its own temperature. Although it has less room for improvement from the side of the cell material, the output power of the PV cell can be increased by adjusting the operating temperature of PV cell.

D. Conversion Efficiency of the Total System

The conversion efficiency of the entire system describes the ability of the system to convert absorbed energy into other forms of energy. Based on the equation of the conversion efficiency in individual PV cells and output power, the energy conversion efficiency of the entire system can be improved at the PV cell itself and using the waste heat from the PV cell. In the system proposed in this article, the energy converted from solar energy by PV is electric energy and thermal energy. In a given period of time, the total energy of sunlight absorbed by the PV cell can be expressed as

$$\begin{aligned} A &= E_{all} \\ &= \int_0^t p_0 dt \\ &= \int_0^t CL(t)\varepsilon\tau S dt \end{aligned} \tag{10}$$

where $L(t)$ is the light intensity at different times. The temperature of the PV cell changes with time, and the converted energy of the PV cell in t seconds is

$$\begin{aligned} B = E_{\text{pv}} &= \int_0^t p_{\text{pv}} dt \\ &= \int_0^t p_0\eta_{\text{pv}}\frac{R_1}{R_0 + R_1} dt \\ &= \int_0^t p_0\eta_0\left[1 - \lambda[T_{\text{pv}}(t) - T_0]\right]\frac{R_1}{R_0 + R_1} dt \end{aligned} \tag{11}$$

where $T_{pv}(t)$ is the temperature of the PV cell at different moments, where the higher the temperature is, the lower the converted energy will be. The energy converted by solar energy includes the electrical energy generated by the PV cell and the electrical energy generated by the TEG. The output power of the TEG primarily depends on the temperature difference at both ends of the TEG, which also changes with time. Therefore, the converted energy of the TEG is expressed as

$$\begin{aligned} C = E_{teg} &= \int_0^t p_{teg} dt \\ &= \int_0^t I_{np}^2 R_a dt \\ &= \int_0^t \left[\frac{S_{np}\left[T_H(t) - T_L(t)\right]}{R + R_a}\right]^2 R_a dt \end{aligned} \tag{12}$$

where $T_H(t)$ and $T_L(t)$ are the temperatures of the hot end and cold end at different moments of TEG, respectively. Specifically, the energy conversion efficiency of the entire system is the ratio of the total energy converted to the total energy absorbed by the system. Thus, the energy conversion efficiency of the entire system is

$$\begin{aligned} \eta &= \frac{E_{\text{pv}} + E_{teg}}{E_{\text{all}}} \times 100\% \\ &= \frac{B + C}{A} \times 100\%. \end{aligned} \tag{13}$$

η can be increased by suppressing T_{pv} of the PV cell to increase E_{pv} or by increasing E_{teg} by increasing the use of waste heat from the system. The maximum overall efficiency of existing research on hybrid energy harvesting systems using PCM has reached 15.88% [24]. Our work will explore new methods to improve efficiency from the aspects of intelligent control of

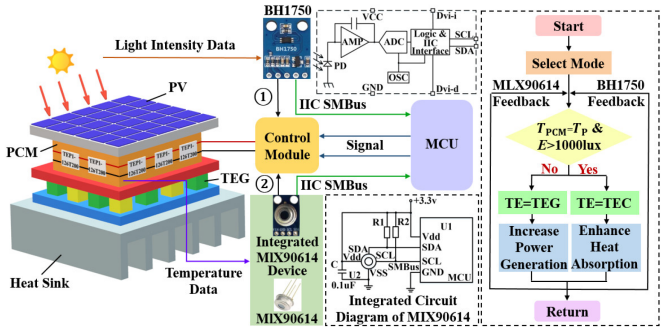

Fig. 4. Intelligent control scheme to delay the PCM phase change time.

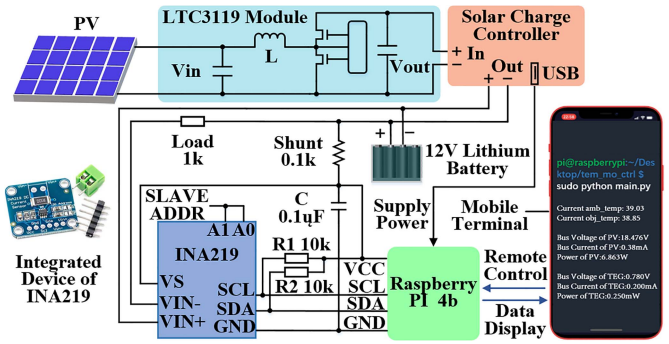

Fig. 5. Schematic diagram of the self-powered system and remote real-time monitoring design. In this case, ports A0 and A1 are the selection ports for the slave address.

phase change delay and design of auxiliary self-powered. Hence, the expected efficiency with our design will be greater.

III. Design of an Intelligent and Efficient Electric Energy Conversion System

PCMs are used in PV-TEG systems with the characteristics of heat absorption and energy storage, creating a new PV-TEG-PCM system. However, the inhibition of PCM on the PV temperature rise is weak in this system structure. To effectively solve the problems of PV heat dissipation and system energy efficiency, an intelligent and efficient self-powered PV-PCM-TE system is proposed in this article. The proposed system can be divided into three primary designs: intelligent control design with time delay phase change, self-supply and remote control, and intelligent mode switching circuit.

A. Intelligent Control Design With Time Delay Phase Change

In this article, we propose an intelligent regulation scheme to extend the phase change time of the PCM shown in Fig. 4. The PCM in the system is attached to the backside of the PV cell. Accompanied by a lot of stored heat, the inherent feature of phase change heat absorption can prevent temperatures from rising in the PV cells. The TEG module is also placed below the PCM module, whose heat source and cold source come from the PCM and heat sink at the bottom, respectively. During phase change heat absorption in the PCM, the temperature difference between the two ends of the TEG tends to be maximized and stable, which is conducive to additional electric energy generation. To fully harvest other waste thermal, a serial TE is integrated into the four sidewalls of the PCM module, whose operating mode is determined by the temperature and light intensity of the PCM. When the temperature of the PCM(T_{PCM}) is not equal to its phase change temperature(T_P), the TE module acts as a TEG in series with the bottom TEG to generate electricity. When the T_{PCM} is equal to its T_P and the light intensity(E) is higher than 1000 lux, the TE module acts as a TEC to cool the PCM module to delay the speed of the phase change of the PCM. This intelligent switching of operating modes requires a temperature monitoring module and a light intensity sensor module to work together. In this article, we use an infrared noncontact thermometer probe MLX90614 to measure the temperature of the PCM in real time and a light intensity sensor BH1750 to measure light intensity. The infrared probe is connected to a pull-up resistor for data transfer with the MCU through an I^2C communication protocol. In the internal light intensity sensor, DVI is the reference voltage port of SDA and SCL, which also supplies the asynchronous reset for the internal register. Based on the photovoltaic effect, a photodiode converts the input light signal into an electrical signal that is amplified by the operational amplifier circuit. The analog voltage is collected by Adc, which will be converted into a 16-bit binary number and finally stored in the internal register. Light intensity data will be transmitted through the I^2C protocol when ports SDA, SCL, VCC, and GND are physically connected to the MCU. After the MCU module receives the measured temperature and light intensity data, matching signals will be transmitted to the peripheral circuit control module to synchronize and control the TE module.

This scheme, which collects light and temperature data in real time and dynamically adjusts the TE operation mode to suppress PV cell heating and prolong the phase change time of the PCM, exploits the ability of the PCM to absorb and store heat and maintain a constant temperature and provides a higher thermoelectric conversion environment for the TEG. In addition, the proposed scheme can use PCM as a heat source and heat sink as a cold source at night and convert self-stored heat into electricity energy through the TEG module at the bottom of the PCM box. The intelligent control design of prolonging the phase change time for PCMs effectively uses the phase change thermostat and energy harvesting properties, which will help to improve the conversion efficiency of the entire PV-PCM-TE system.

B. Power Monitoring and Self-Powered Design With a Wireless Transceiver

A Raspberry Pi 4b hardware board is primarily in charge of the instruction transfer of the control module and exchange of bus data, which is powered by an external power supply with a voltage of 5 V in the experiment. However, its consumed power is high, and thus, combining the advantages of energy harvesting by converting light and heat energy into electricity in this article, we propose a self-powered design for the MCU, as shown in Fig. 5, which can effectively reduce the energy consumption

demand of the entire PV-PCM-TE system. Because the voltage directly generated by PV cells is unstable, it is easily disturbed by the external environment, light, and other factors. Based on an internal positive feedback technique applied in the amplifier circuit, a dc–dc boost component is used to generate a stable output voltage. In the front-end circuit design, the regulated output voltage of 12 V is obtained using the core module LTC3119 in the proposed design with energy originating from the PV cell. Then, the generated stable voltage of 12 V is supplied to the solar controller to directly perform electricity energy distribution management. The surplus part of the power is stored in the lithium battery at a voltage of 12 V, which is protected by the proposed lithium battery overcharge control circuit. The power of the Raspberry Pi 4b module is connected to the solar controller through USB, completely enabling the load to be self-powered. To master the usage of electricity in a self-power system, the bidirectional current and power are measured by an INA219 sensor. By measuring the voltage drop across the shunt resistor and the voltage supplied by the shunt, the current and power consumed by the load are determined. Next, the acquired power data are sent to the MCU through I^2C communication. Finally, we design an electric energy and remote-control app on a cell phone terminal display for portable control. Linux commands from the cell phone app are transmitted to the Raspberry Pi via wireless LAN to gather the energy data. Then, the Raspberry Pi module uses the wireless transceiver unit to transmit the electric energy data to the app. Without batteries and data cables, the proposed system is more convenient when monitoring the power generation status of PVs in real time, which effectively achieves both low energy consumption and portability, and thus facilitates outdoor control.

C. Intelligent Switching Circuit Control for TE Mode

As shown in Fig. 4, the serial TE array is integrated into the sidewall of the PCM module in the scheme. The working mode in the TE array switches between TEC and TEG, where the operating time directly exerts an influence on the final efficiency of the entire power conversion system. Thus, we propose a fast and accurate TE mode switching circuit with intelligent control to maximize the phase change time in PCM. The design process is as follows. First, the temperature and light intensity data obtained from MLX90614 and BH1750 are transmitted to the Raspberry Pi, as well as the corresponding signal after the program judgment. As shown in Fig. 6, to achieve fast synchronous circuit switching, the signals sent by the Raspberry Pi will be synchronized by a signal inversing circuit, which will send two opposite signals to the gates of NMOS1 and NMOS2 synchronously. The circuit strobe is jointly realized by the ON-OFF of the NMOS and SGM3001 analog switch modules. The operating mode of both the TEG and TEC will be selected according to the judgment criteria given in part A to complete the circuit switching. When the system temperature measurement module detects that the temperature of the PCM is equal to that of the phase change and the light intensity sensor verdict is higher than 1000 lux, a command will be transmitted to control NMOS2 on and NMOS1 off by the Raspberry Pi, and COM in SGM3001

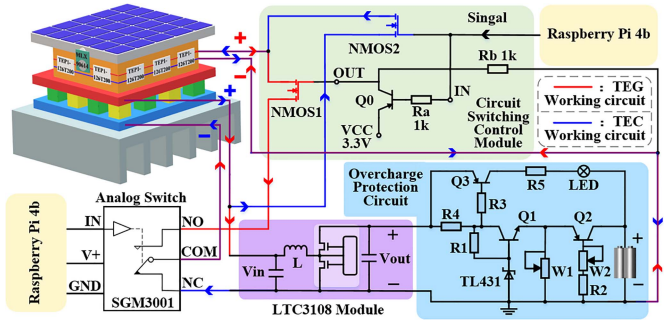

Fig. 6. TE operating mode switching and circuit protection in phase change energy conversion systems. The red circuit diagram shows the TEG operating mode circuit, and the blue circuit shows the TEC operating mode circuit.

is used to connect to the interface of NC. At this time, the TEC mode starts. The power stored in the battery will supply the TE module to cool down the PCM module; thus, the phase change time is extended by increasing the heat absorption for the PCM. Thus, the power of the TEC comes from the harvested and stored waste heat, which is a completely self-powered working mode. In other cases, the system will control NMOS1 to turn on and NMOS2 to turn OFF, and then, the COM terminal of SGM3001 will be switched to "NO." The serial TE module in TEG mode is connected with the TEG at the bottom. Regulated by the boost module LTC3108, the stable output voltage is obtained from the converted power. After the overcharge protection circuit, it will be stored in a lithium battery at 5 V as a back-up power supply for the TEC working mode. In the overcharge protection circuit, R1, Q1, W1, and TL431 form a precision adjustable voltage regulator circuit to ensure voltage stability. To ensure constant current, an adjustable constant current circuit consisting of Q2, W2, and R2 is designed. The circuit is also designed with a charging feedback function consisting of Q3, R3, R4, R5, and LED. When the battery is charged, the charging current will decrease with increasing voltage at both terminals. As a result, the voltage drop on R4 will decrease with the cutoff state of Q3, leading to the closed LED charging indicator, which indicates that the battery is full to prevent overcharging.

IV. Results and Discussion

A. System Environment Setup

To verify the advantages of the PV-PCM-TE system proposed in this article, PV-TEG-PCM, PV-PCM-TEG, and PV-PCM-TE systems were built for experimental comparison. A PV cell with a model of CY3210 and voltage of 12 V was used. A TEP1-126T200 TEG was used in the experiment due to its high temperature resistance. We used paraffin wax with a phase change temperature of 38 °C as the PCM. To alleviate the problem of low thermal conductivity of PCM, a container box with dimensions of 150 mm×150 mm×50 mm was customized to accommodate the PCM powder. As shown in Fig. 7(a), the container box of PCM was made of purple copper with neatly arranged top-down heat teeth on the lid to ensure better and more uniform heat transfer. Before the experiment, the container

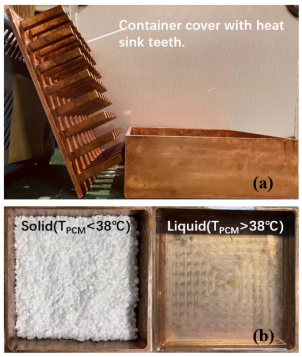

Fig. 7. (a) PCM container box. (b) PCM performance test.

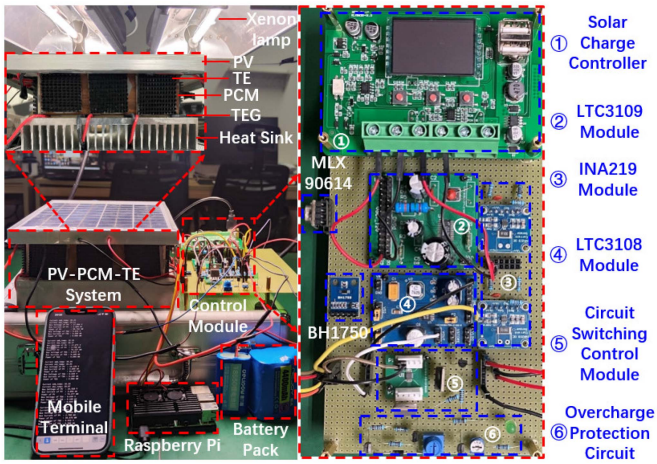

Fig. 8. System experimental setup diagram.

box with PCM was placed on the heating table for testing the phase change temperature. Experimental results are shown in Fig. 7(b). The PCM started to melt slowly from the solid to liquid state when the temperature reached 38 °C. The entire phase change time continued for approximately 30 mins. After the heating table was turned off, the PCM slowly solidified when the temperature dropped to 38 °C. Approximately 32 min later, all of the PCM returned to being a solid and adhered to the container again.

The experimental setup of the proposed system is shown in Fig. 8. TE arrays with 11 modules in series connection are assembled around the PCM container box, where a MLX90614 is placed in the center to measure temperature in real time. To reuse waste heat, nine TEGs in series contained an energy conversion module that was placed between the PCM container box and the heat sink. The integrated assembly of temperature monitoring, circuit control, MCU, and other modules at the periphery of the experiment are shown on the right side of Fig. 8, where two INA219s are used to obtain the energy conversion power of PVs and TEGs, and a BH1750 is used to measure the light intensity. The Raspberry Pi is used to receive data and send instructions. All data visualizations and manipulations are performed through the APP Termius in cell mobile. To make the experiment more effective, a xenon lamp is used instead of

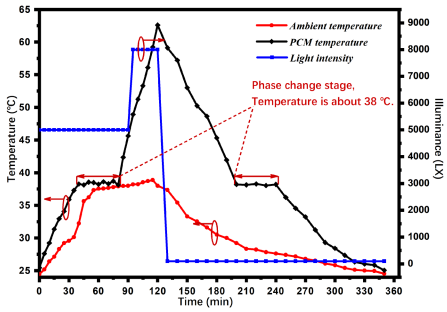

Fig. 9. PCM performance testing and environmental documentation.

another light source. Thus, the light intensity during the experiment can be characterized by changing the distance between the PV and the xenon lamp. To test the state of the waste heat utilization process, the experimental system requires a total of five hours with the xenon lights on to simulate daytime for the initial two hours. The later three hours are spent with the xenon lights OFF to simulate nighttime. The light intensity variation and real-time ambient temperature during the experiment are shown in Fig. 9. The xenon lamp operates at a light intensity of 5000 lux in the beginning of 1.5 h and then increases to 8000 lux. The phase change temperature of the PCM is approximately 38 °C, which remains relatively constant throughout the phase change. The ambient temperature increases rapidly in the initial stage and then increases slightly when the xenon lamp intensity increases, reaching a maximum temperature of 38.6 °C.

B. Intelligent Working Process

Based on the system hardware test platform in Fig. 8, the intelligent working process of our proposed system is as follows: During the beginning of one day, the temperature of the PCM continues to rise under light. The illumination sensor BH1750 and infrared temperature sensor MLX90614 in the system will respectively collect the current light intensity and PCM temperature, and provide real-time feedback to Raspberry Pi 4b. When the light intensity is greater than 1000 lux (indicating daytime) and the temperature of the PCM is equal to 38 °C (phase change temperature), Raspberry Pi 4b will send commands to the control circuit module based on the feedback information. The control circuit will switch the operation of the circuit according to instructions, and the TE module will be converted into TEC to cool the PCM. At this stage, due to the ability to maintain a constant temperature when the PCM melts, the TE module used as a TEC for cooling removes the heat absorbed by the PCM while prolonging the phase change time of the PCM, ultimately increasing the power generation of PV and TEG. Similarly, when the temperature is above 38 °C, Raspberry Pi 4b receives the feedback information from the sensor and sends corresponding instructions to the control circuit module. After receiving instructions, the control circuit changes the operation mode of the circuit, and the TE module is switched to TEG and connected in series with the TEG at the bottom of the PCM to generate electricity together. At night, TE module itself consumes a certain amount of energy as TEC. If TEC is only

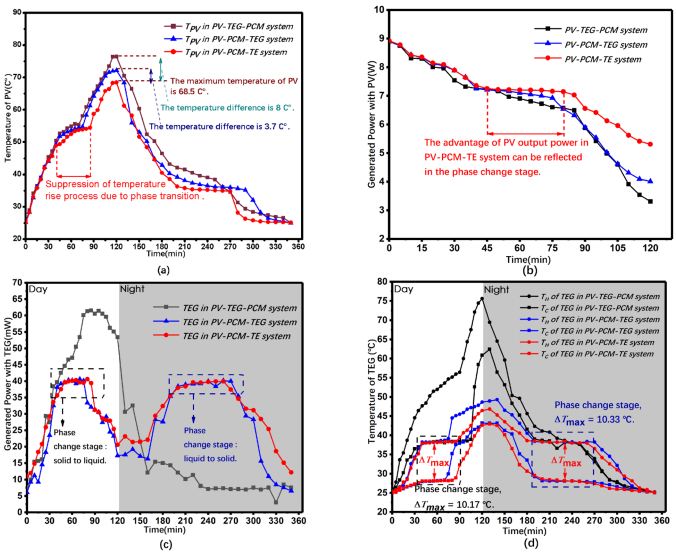

Fig. 10. (a) PV temperature. (b) PV output power. (c) TEG output power. (d) Temperature on both sides of the TEG.

used to increase the temperature difference of TEG at the bottom of PCM container box, it will not be able to make ends meet. So when Raspberry Pi 4b detects an intensity of light less than 1000 lux, it will control the TE module to act as TEG throughout the night, generating electricity from the latent heat in the PCM.

C. Measured Temperature and Generated Power

Fig. 10(a) shows the temperature changes of the PV panel in three different systems (PV-TEG-PCM, PV-PCM-TEG, and PV-PCM-TE) under the same experimental environment. The PV temperature of all three systems increased markedly initially and then slowed after approximately 40 mins. After 120 min, the xenon lamp was turned off, and the PV temperature of all three systems started to decrease. Approximately 190 min later, this trend was followed by another slowing of the rate of change of the temperature. Both of these decreases in the rates of change of temperature are due to the temperature reaching the phase change temperature of the PCM, when the PCM absorbs heat at a stable temperature, which keeps the PV panel at the same temperature. In particular, the proposed PV-PCM-TE system maintains a longer period of constant temperature than the other two systems, thus more effectively suppressing increasing temperature in the PV cell. These results demonstrated that the intelligent switching of TE operation mode can effectively improve the ability to suppress the PV temperature rise in the proposed PV-PCM-TE system. Under the same external conditions, the maximum temperature of the PV cell with the proposed system is only 68.5 °C, which is 8 °C and 3.7 °C lower than that with the PV-TEG-PCM and PV-PCM-TEG systems, respectively. Fig. 10(b) shows the generated PV power measured by IN219 for the three systems within 0–120 min with a high temperature range. The PV power of the three systems continues to decrease due to the continuous increase in the junction temperature. The decreasing trend of PV power is slowed by approximately 50 min, which is also due to the phase change occurring for PCM. The decreasing trend of the PV-PCM-TEG and PV-PCM-TE systems is markedly slowed because the PCM is physically closer to the PV in the proposed structure. The PV output power of the proposed PV-PCM-TE system remains constant, even during phase change, which is near 7.2 W. The phase change time is delayed to 42 min, which is 40% higher than that of the PV-PCM-TEG of 30 min. The effectiveness of intelligent phase change time control design for PCM is thus again confirmed. Synchronously, the electrical energy in TEC mode comes from the self-powered network, which also improves the conversion efficiency of the entire system.

Fig. 10(c) describes the power generated by the TEG of the three systems. Because the experiment was performed with a xenon lamp with constant intense light intensity, the temperature of the PV cell showed a rapid increase. As a result, the TEG temperature difference between the three systems continued to increase rapidly at the beginning process. After the experiment was conducted for approximately 40 min, the TEG output power of the PV-PCM-TEG and PV-PCM-TE systems reached a maintained peak, while that of the PV-TEG-PCM system continued to increase, which was much higher than that of the former two systems. This phenomenon is caused by the fact that the former two systems use PCM as the heat source of TEG, while the latter uses PCM as the cold source. As the heat source for the TEG, the PCM that is closely attached to the PV will result in a maximum and constant power output time period for the TEG module during the phase change stage. It can also be seen that the PV-PCM-TE system proposed in this article significantly extends the TEG constant power output time due to the intelligent switching technology of the TE operation mode. Fig. 10(d) shows the temperature change profiles of both sides of the TEG for the three system structures. At the stage of temperature rise on both sides, the temperature difference between the two sides of the TEG in the PV-TEG-PCM system increases continuously at first and then increases abruptly when the temperature at the cold end reaches approximately 38 °C. The temperature difference between the TEG in the PV-PCM-TEG and PV-PCM-TE systems will tend towards a maximum value and remain stable when the temperature at the hot end reaches approximately 38 °C, and the latter stays longer. The temperature difference between the two sides of the TEG in the PV-TEG-PCM system decreases until it is near the temperature drop on both sides. The temperature difference between the two sides of the TEG in the PV-PCM-TEG and PV-PCM-TE systems increases continuously and reaches a maximum value when the hot end temperature drops to approximately 38 °C and remains stable. This result indicates that the PCM has different effects when placed in different positions in the system, and the PCM can make the TEG have a stable output over a period of time and have the ability to generate electricity at night. In general, the proposed PV-PCM-TE system in this article can generate the maximum and constant output power of a TEG for a longer period of time compared to the PV-PCM-TEG system, thus improving the waste heat conversion efficiency of

TABLE I
PERFORMANCE COMPARISON OF RELATED STUDIES

/	Yin et al. [13] 2019	Wang et al. [14] 2021	J. Darkwa et al. [23] 2019	Milad et al. [24] 2021	**This work 2022**
Energy Conversion System	PV-TEG	PV-TEG	PV-TEG-PCM	PV-PCM-TEG	**PV-PCM-TE**
Technology	Optimal load resistance of the TE module	Intelligent power track switching and efficient thermal management	Adjusting PCM thickness	Control variables and simulate	**Self-supply and remote regulation mechanism**
Analysis Type	Experiment	Experiment	Experiment	Simulation	**Experiment**
Cooling Method	Water	Heatsink	PCM	PCM	**PCM**
Intelligent Control	×	√	×	×	√
Self Energy Supply	×	×	×	×	√
Battery Protection	×	√	×	×	√
Working Hours: Day and Night	×	×	×	√	√
Suppressed Temperature for PV	2.5℃	4℃	2.2℃	7.71℃	**8℃**
Maximum Output Power	1.51W	7.02W	8.5W	8.68W	**8.924W**
Maximum Energy Conversion Efficiency	18.1%	21.6%	11.50%	15.88%	**30.26%**

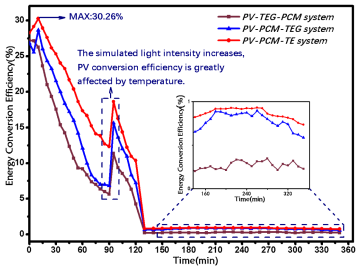

Fig. 11. Transient energy conversion efficiency of the three systems.

PCMs. In addition, the system will have a long-term and stable energy supplement at night, which contributes to the overall improvement of energy utilization efficiency.

D. Performance Comparison

Fig. 11 shows a comparison of the energy conversion efficiency of the PV-TEG-PCM, PV-PCM-TEG, and PV-PCM-TE systems calculated from the experiment. The energy conversion efficiency quickly reached its peak in approximately 13 min due to the not yet dominant heat gathered by the PV nodes at the beginning of the experiment. However, the energy conversion efficiency begins to decrease as the PV temperature increases when lit. The energy efficiency of the proposed system decreases more slowly than that of PV-PCM-TEG at this time, which indicates that the PV temperature is better suppressed by the proposed system. The influence of temperature on the photovoltaic effect of PV in PV-PCM-TE is less than that of the PV-PCM-TEG system. At 90 min, a small increase in the energy conversion efficiency of the three systems occurs due to the experimental enhancement of the light intensity to test the high-intensity reliability with the working PV. After 130 min, the conversion efficiency of the three systems drops to the minimum along with the entering night operation mode. The inset in Fig. 11 shows that the PV-PCM-TE system has the highest energy utilization at night, primarily because the system structure switches the TE module on the side of the PCM into the TEG working mode, and the bottom TEG in series will participate in energy conversion together, which maximizes the use of the heat stored in the PCM and improves the energy conversion efficiency of the system. The proposed system structure thus has a maximum energy conversion efficiency of 30.26% due to the use of intelligent switching circuits and self-supply design technology. Its average conversion efficiency is improved by 43.15% relative to the PV-TEG-PCM system and 21.68% compared to the PV-PCM-TEG system. The system proposed in this article can thus overcome the defect of reduced conversion efficiency of PV under high temperature but can also harvest and use energy at night, maximizing the overall energy conversion process.

Table I also compares the performances of the proposed system and the PV-TEG, PV-TEG-PCM, and PV-PCM-TEG systems in recent years. The three systems with PCM have a clear advantage in terms of maximum output power (>8 W), which is stronger than that in water-cooled and heat sink cooling systems. Using self-power, a phase change extension, intelligent monitoring, and real-time regulation of the working mode technologies, the PV temperature was effectively reduced by 8 °C in the proposed system, and the maximum output power reached 8.924 W with a maximum energy conversion efficiency of 30.26%. The system also improves the constant power energy output of the TEG due to a relatively longer phase change time of the PCM. The proposed system makes full use of PCM for heat dissipation, energy storage during the daytime, and the energy absorbed for heat storage at night. Thus, the performance of the proposed system is better than other similar systems.

V. CONCLUSION

In this article, a PV-CPM-TE system based on a long delay phase change is designed and verified. To enhance the ability of PCM to suppress the temperature rise in PV, the extension design of phase change time, a self-powered MCU, and intelligent switching control for TE mode were proposed to

improve energy utilization. Using the PCM auxiliary energy supply technique, the energy conversion can be improved, even at night. Three sets of comparison experiments are conducted between the PV-TEG-PCM, PV-PCM-TEG, and PV-PCM-TE systems. Experimental results show that the temperature of the PV cell is better controlled in the proposed system compared with the PV-TEG-PCM system, achieving a temperature drop of 8 °C and a 43.15% increase in energy conversion efficiency. Compared with the PV-PCM-TEG system, the phase change time of PCM is extended by 15 min, and the temperature of PV is reduced by 3.7 °C. The output power of PV can reach up to 8.924 W with the peak energy conversion efficiency up to 30.26%. The experiment performed in this article shows that the proposed system makes full use of the heat-absorption and energy-storage properties of PCM, effectively suppressing any temperature rise in the PV panel and markedly improving the energy conversion efficiency of the entire system.

REFERENCES

[1] B. Aksanli and T. S. Rosing, "Human behavior aware energy management in residential cyber-physical systems," *IEEE Trans. Emerg. Topics Comput.*, vol. 8, no. 1, pp. 45–57, Jan.–Mar. 2020.

[2] N. M. Shatar, M. A. A. A. Rahman, S. A. Z. S. Salim, M. H. M. Ariff, M. N. Muhtazaruddin, and A. K. A. Badlisah, "Design of photovoltaic-thermoelectric generator (PV-TEG) hybrid system for precision agriculture," in *Proc. IEEE 7th Int. Conf. Power Energy*, 2018, pp. 50–55.

[3] Y. Li, N. Fatima, M. Ahmad, G. Jabeen, and X. Li, "Dynamic long-run connections among renewable energy generation, energy consumption, human capital and economic performance in Pakistan," in *Proc. 4th Int. Conf. Power Renew. Energy*, 2019, pp. 152–156.

[4] D. Gielen, F. Boshell, D. Saygin, M. D. Bazilian, N. Wagner, and R. Gorini, "The role of renewable energy in the global energy transformation," *Energy Strategy Rev.*, vol. 24, pp. 38–50, 2019.

[5] M. Z. Hakuba et al., "Earth's energy imbalance measured from space," *IEEE Trans. Geosci. Remote Sens.*, vol. 57, no. 1, pp. 32–45, Jan. 2019.

[6] F. Deng, L. Ma, X. Gao, and J. Chen, "The MR-CA models for analysis of pollution sources and prediction of PM2.5," *IEEE Trans. Syst., Man, Cybern., Syst.*, vol. 49, no. 4, pp. 814–820, Apr. 2019.

[7] E. Khodabandeh, M. R. Safaei, S. Akbari, O. A. Akbari, and A. A. Alrashed, "Application of nanofluid to improve the thermal performance of horizontal spiral coil utilized in solar ponds: Geometric study," *Renew. Energy.*, vol. 122, pp. 1–16, 2018.

[8] M. M. Sarafraz, I. Tlili, Z. Tian, M. Bakouri, and M. R. Safaei, "Smart optimization of a thermosyphon heat pipe for an evacuated tube solar collector using response surface methodology (RSM)," *Phys. A Statist. Mech. Appl.*, vol. 534, 2019, Art. no. 122146.

[9] U. A. Saleh, S. A. Jumaat, M. A. Johar, and W. A. W. Jamaludin, "Photovoltaic-thermoelectric generator monitoring system using arduino based data acquisition system technique," in *Proc. IEEE Int. Conf. Artif. Intell. Eng. Technol.*, 2021, pp. 1–6.

[10] Y. Tian and C. Y. Zhao, "A review of solar collectors and thermal energy storage in solar thermal applications," *Appl. Energy.*, vol. 104, pp. 538–553, 2013.

[11] P. Saxena and N. E. Gorji, "COMSOL simulation of heat distribution in perovskite solar cells: Coupled optical–electrical–thermal 3-D analysis," *IEEE J. Photovolt.*, vol. 9, no. 6, pp. 1693–1698, Nov. 2019.

[12] Ö. F. Keser, B. İdare, B. Bulat, and A. Okan, "The usability of PV-TEG hybrid systems on space platforms," in *Proc. Int. Conf. Recent Adv. Space Technol.*, 2019, pp. 109–115.

[13] Q. L. Yin and Y. Xuan, "Experimental optimization of operating conditions for concentrating photovoltaic-thermoelectric hybrid system," *J. Power Sources*, vol. 422, pp. 25–32, May 2019.

[14] Z.-H. Shen et al., "Improving the energy-conversion efficiency of a PV-TE system with an intelligent power-track switching technique and efficient thermal-management scheme," *IEEE Trans. Compon. Packag. Manuf. Tech.*, vol. 11, no. 6, pp. 963–973, Jun. 2021.

[15] Z. Y. Luo, N. Zhu, P. F. Hu, F. Lei, and Y. X. Zhang, "Simulation study on performance of PV-PCM-TE system for year-round analysis," *Renew. Energy*, vol. 195, pp. 263–273, 2022.

[16] M. Taqi and M. Mahdi, "Novel mathematical modeling, performance analysis, and design charts for the typical hybrid photovoltaic/phase-change material (PV/PCM) system," *Appl. Energy*, vol. 315, 2022, Art. no. 119027.

[17] E. H. Amalu and A. Fabunmi, "Thermal control of crystalline silicon photovoltaic (c-Si PV) module using docosane phase change material (PCM) for improved performance," *Sol. Energy*, vol. 234, pp. 203–221, 2022.

[18] Ç. Yıldız, M. Arıcı, and S. Nizetic, "Natural convection of molten PCM in a finned enclosure used in PV/PCM systems," in *Proc. Int. Conf. Smart Sustain. Technol.*, 2020, pp. 1–6.

[19] K. Ismail and M. Goncalves, "Thermal performance of a PCM storage unit," *Energy Convers. Manage.*, vol. 40, pp. 115–138, 1999.

[20] X. Sui, W. Li, Y. Zhang, and Y. Wu, "Theoretical and experimental evaluation of a thermoelectric generator using concentration and thermal energy storage," *IEEE Access*, vol. 8, pp. 87820–87828, 2020.

[21] J. Maciej, B. Marta, and C. Marceli, "Experimental investigation of thermoelectric generator (TEG) with PCM module," *Appl. Thermal Eng.*, vol. 96, pp. 527–533, 2016.

[22] T. Truong, V. Nguyen, and O. Takahito, "Theoretical and experimental investigation of a thermoelectric generator (TEG) integrated with a phase change material (PCM) for harvesting energy from ambient temperature changes," *Energy Rep.*, vol. 6, pp. 2022–2029, 2020.

[23] J. Darkwa, J. Calautita, D. Dub, and G. Kokogianakis, "A numerical and experimental analysis of an integrated TEG-PCM power enhancement system for photovoltaic cells," *Appl. Energy*, vol. 248, pp. 688–701, 2019.

[24] N. Milad, M. Ziapour, and G. Mohammad, "Improvement of photocells by the integration of phase change materials and thermoelectric generators (PV-PCM-TEG) and study on the ability to generate electricity around the clock," *J. Energy Storage*, vol. 36, 2021, Art. no. 102384.

[25] T. F. Cui and Y. M. Xuan, "Experimental investigation on potential of a concentrated photovoltaic-thermoelectric system with phase change materials," *Energy*, vol. 122, pp. 94–102, 2017.

[26] Y. Y. Tian, A. B. Liu, J. L. Wang, and Y. J. Zhou, "Optimized output electricity of thermoelectric generators by matching phase change material and thermoelectric material for intermittent heat sources," *Energy*, vol. 223, 2021, Art. no. 121113.

[27] A. Liu, J. Zou, Z. Wu, Y. Wang, Y. Tian, and H. Xie, "Enhancing the performance of TEG system coupled with PCMs by regulating the interfacial thermal conduction," *Energy Rep.*, vol. 6, pp. 1942–1949, 2020.

[28] L. E. Bell, "Cooling, heating, generating power, and recovering waste heat with thermoelectric systems," *Science*, vol. 321, pp. 1457–1461, 2008.

[29] S. Asaadi, S. Khalilarya, and S. Jafarmadar, "Numerical study on the thermal and electrical performance of an annular thermoelectric generator under pulsed heat power with different types of input functions," *Energy Convers. Manage.*, vol. 167, pp. 102–112, 2018.

[30] J. Kang, D. Wee, and S. Bang, "Approximate formulae for thermal resistance matching of thermoelectric coolers operating at room temperature," *Case Stud. Thermal Eng.*, vol. 23, 2021, Art. no. 100799.

[31] M. Lallart, L. V. Phung, and B. Massot, "Transformer-free, off-the-shelf electrical interface for low-voltage DC energy harvesting," *IEEE Trans. Ind. Electron.*, vol. 65, no. 7, pp. 5580–5589, Jul. 2018.

[32] U. A. Saleh, S. A. Jumaat, M. A. Johar, and W. A. Jamaluddin, "Performance of the hybrid photovoltaic-thermoelectric generator (PV-TEG) system under malaysian weather conditions," in *Proc. IEEE Conf. Energy Convers.*, 2021, pp. 11–16.

[33] [Online]. Available: https://www.alibaba.com/product-detail/SIZE-40-40mm-TEP1-126T200-tep_1600794271814.html?spm=a2700.7724857.0.0.1a707d0684Tque

[34] A. Bria, B. Raillani, D. Chaatouf, M. Salhi, S. Amraqui, and A. Mezrhab, "Numerical investigation of the PCM effect on the performance of photovoltaic panels; comparison between different types of PCM," in *Proc. 2nd Int. Conf. Innov. Res. Appl. Sci., Eng. Technol.*, 2022, pp. 1–5.